Imidazolium-Based Ionic Liquids in Water: Assessment of Photocatalytic and Photochemical Transformation

UNIVERSITÀ DEGLI STUDI DI TORINO

Imidazolium-based ionic liquids in water: Assessment of photocatalytic and photochemical transformation

Paola Calza[a], Davide Vione[a]*, Debora Fabbri[a], Riccardo Aigotti[b], and Claudio Medana[b]

[a] *Department of Chemistry, University of Torino, via P. Giuria 5, 10125 Torino, Italy*

[b] *Department of Molecular Biotechnology and Health Sciences, University of Torino, via P. Giuria 5, 10125 Torino, Italy*

** Corresponding author. Phone: +39-011-6705296; Fax: +39-011-6705242:*

E-mail: davide.vione@unito.it

Abstract

The photoinduced transformation of two ionic liquids, 1-methylimidazolium hydrogensulfate (HMIM) and 1-ethyl-3-methylimidazolium hydrogensulfate (EMIM) was investigated under photocatalytic conditions in the presence of irradiated TiO_2. We monitored substrate disappearance, transformation products (TPs), degree of mineralization and toxicity of the irradiated systems. Acute toxicity measures suggested in both cases the occurrence of more toxic TPs than the parent molecules. A total of five TPs were detected by HPLC-HRMS from HMIM and nine from EMIM. Complete mineralization and stoichiometric release of nitrogen was achieved for both compounds within 4 h of irradiation. The photochemical transformation kinetics and pathways in surface waters (direct photolysis and indirect photoreactions) were studied for EMIM, to assess its persistence in sunlit water bodies such as rivers or lakes. Environmental phototransformation would be dominated by direct photolysis, with half-life times of up to one month under fine-weather conditions.

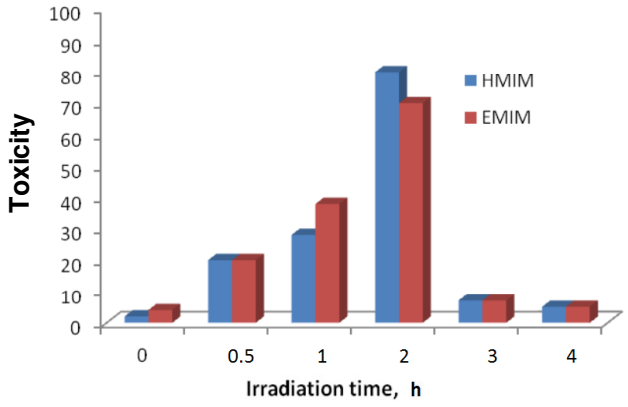

Introduction

Ionic liquids (ILs) are potential alternative solvents, promoted as “green chemistry” replacements to traditional solvents used in industry. Recently, they were included in the list of the so-called "contaminants on the horizon".[1] The considerable interest toward these compounds relies on their low vapor pressures and flammability, chemical and thermal stability, high ionic conductivity, wide electrochemical potential window and ability to behave as catalysts. The ILs chemical structures typically involve a cationic or anionic polar headgroup with accompanying alkyl side chains. By changing the structure of this group (e.g. by varying the alkyl chain or the core), it is possible to modify the physical properties and to influence the biological features. For the possibility to tune their properties as a function of the chemical structure, ILs can be defined as “designer solvents”.[2]

In view of the growing industrial interest towards ILs, many risk scenarios should be taken into account including the IL occurrence in industrial effluents, which might affect aquatic ecosystems. Kalcikova et al. compared the ecotoxicity of one of these ionic liquids (1-butyl-3-methylpyridinium dicyanamide) to other commonly used solvents, finding it to be toxic to all organisms tested and more toxic than common solvents.[3] Only a few environmental data for these new “green solvents” are presently available, but their potential ability to pose a threat to aquatic and terrestrial ecosystems should be tested. While not volatile, most ionic liquids are highly water-soluble and chemically and thermally stable, which creates the potential for access to and persistence in the environment.

The environmental impact of ILs and their actual “greenness” have been assessed in a series of interdisciplinary studies.[4,5,6,7] These have underlined the importance of a preventive evaluation in the phase of ILs design, because their structure affects the pertinent technological, toxicological and eco-toxicological properties. In particular, the risk associated to ILs should be analyzed by taking into account several factors, such as release, biodegradability, biological activity and uncertainty of action compared to traditional solvents. Many bioassays have been put forward using fish, plants, algae, soil invertebrates, mussels, crustaceans and bacteria (as well as toxicity studies at cellular and sub-cellular levels) for detecting the IL toxic effects in terrestrial and aquatic ecosystems.[8,9,10,11,12,13,14,15,16,17,18,19,20] Current data show that ILs are often toxic and that their toxicity varies considerably across organisms and trophic levels.[21,22,23] Many ILs could thus deeply affect aquatic and terrestrial organisms, and their toxic effects rise by increasing the alkyl chain length of the cation. For the most common classes of ILs, the main contribution to the toxicity is basically due to the cation moiety, although also the anion could significantly contribute towards some test species. Such results (increasing toxicity by increasing lipophilicity) have been confirmed

in cellular and subcellular tests. The introduction of polar groups into the alkyl chains has been shown to decrease toxicity and increase biodegradation, suggesting the possibility of tailoring the chemical structures to produce more environmentally friendly compounds.

The low biodegradability and considerable ecotoxicity of some ILs are the reasons why we should prevent their leakage into the environment, choosing effective means of removal and recovery from wastewater as well as minimizing their presence in such a matrix. Against this background we studied two ILs, 1-methylimidazolium hydrogensulfate (HMIM) and 1-ethyl-3-methylimidazolium bisulfate (EMIM), investigating the feasibility of their advanced oxidative removal by heterogeneous photocatalysis. In the case of EMIM it was also assessed the surface-water photofate, to estimate photochemical persistence. The identification of transformation products (TPs) is a crucial aspect because, in addition to providing important information on the mechanism of degradation, the formed TPs may have a very different impact on the environment compared to the parent molecules. To our knowledge, this is the first study about the photochemical and photocatalytic transformation of HMIM and EMIM.

Experimental section

Materials

TiO_2 P25 was used as photocatalyst, after being subjected to irradiation and washings with ultrapure water to eliminate the potential interference caused by adsorbed ions such as chloride, sulfate and sodium. When used, the TiO_2 loading was always 200 mg L^{-1}.

1-Methylimidazolium hydrogensulfate (HMIM, 98%), 1-ethyl-3-methylimidazolium hydrogensulfate (EMIM, 98%), N-ethylenformamide (98%), methanol (≥99.9%), acetonitrile (≥99.9%), formic acid (99%), NaCl (≥ 99.5%), NaOH (99%), hydrogen peroxide (35% w/w), antraquinone-2-sulfonic acid, sodium salt (AQ2S, 98%) and furfuryl alcohol (98%) were purchased from Sigma Aldrich (Milan, Italy). Rose Bengal was purchased from Alfa Aesar (Karlsruhe, Germany).

Irradiation procedures

Direct and indirect photolysis

Five milliliters of aqueous solutions, containing 20 μM of EMIM were introduced into cells of

Pyrex glass (cylindrical, 4.0 cm diameter, 2.3 cm height) and subjected to irradiation. In these and all the other experiments the initial pH of the solutions was set to around 7 by using NaOH. Different lamps were used, depending on the performed experiments.

A 40 W Philips TL K05 lamp with maximum emission at 365 nm was used to assess the triplet sensitization by irradiated AQ2S, where the AQ2S triplet state (^{3}AQ2S*) was employed as proxy of the triplet states of chromophoric dissolved organic matter (^{3}CDOM*).[24] A 20 W Philips TL 01 RS lamp with emission maximum at 313 nm was used to excite H_2O_2 and produce hydroxyl ($^{\bullet}$OH) radicals, as well as to study the reactivity of EMIM with carbonate radicals ($CO_3^{-\bullet}$). Measures of reactivity with singlet oxygen ($^1O_2$) were performed using a lamp Philips TL D 18W/16 with emission maximum at 545 nm. The dye Rose Bengal (10 μM initial concentration) was chosen as the $^1O_2$ source. The temperature of the irradiated solutions in these and other experiments was around 30°C.

Photocatalysis

The irradiation experiments were carried out in Pyrex glass cells, filled with 5 mL of a suspension containing the analyte (10 mg/L) and the TiO_2 catalyst (200 mg/L). Samples were subjected to different irradiation times (ranging from 5 min to 4 h), using the 40 W Philips TL K05 lamp. After illumination, the entire content of each cell was filtered through a 0.45 μm filter and then analyzed. The lamp irradiance over the irradiated solutions was around 30 W/m^2 in the wavelength range of 290-400 nm (measured with a power meter from CO.FO.ME.GRA., Milan, Italy). At the pH 7 of the irradiation experiments, approximately half of HMIM (pKa~7)[5,10,21] would occur as the positively charged protonated species, and the other half as the deprotonated neutral form. No buffers were used to control the pH, because TiO_2 strongly suffers from the occurrence of either organic or inorganic additives that inhibit photodegradation, which operate by scavenging reactive species or by competing with the substrate(s) for adsorption on the oxide surface.[25]

Analytical procedures

HPLC-UV

EMIM and HMIM were monitored with a Merck-Hitachi chromatograph equipped with Rheodyne injector (50 μL sample loop), L-6200 and L-6200A pumps for high-pressure gradients, L-4200 UV-Vis detector, and a RP C18 column (Lichrochart, Merck, 12.5 cm x 0.4 cm, 5 μm packing). Isocratic elution (0.2 mL/min flow rate) was carried out with 95% of 0.1 M sodium hexanesulphonate in water (pH 3.5) and 5% acetonitrile. Retention times were 6.71 (HMIM) and 8.12 (EMIM) min, the

detection wavelength was set at 210 nm.

Liquid Chromatography - Mass Spectrometry

The chromatographic separations, monitored using a MS analyzer, were run on a Phenomenex Luna C18 (2) column, 150 × 2.1 mm × 3 µm particle size (Phenomenex, Bologna, Italy), using an Ultimate 3000 HPLC instrument (Dionex, Thermo Scientific, Milan, Italy). Injection volume was 20 µL and flow rate 200 µL/min. A gradient mobile phase composition was adopted, consisting of methanol/formic acid 0.05% v/v in water (when run in ESI(+)) or acetonitrile/ammonium acetate 0.1 mM (ESI(−)). The eluent composition was varied from 5/95 to 100/0 in 40 min.

A LTQ Orbitrap mass spectrometer (Thermo Scientific, Milan, Italy) equipped with an atmospheric pressure interface and an ESI ion source was used. The LC column effluent was delivered into the ion source using nitrogen as both sheath and auxiliary gas. The tuning parameters adopted for the ESI source were capillary voltage 37.00 V and tube lens 65 V. The source voltage was set to 3.5 kV and the heated capillary temperature was maintained at 275°C. The acquisition method was optimized beforehand in the tuning sections for the parent compound (capillary, magnetic lenses and collimating octapole voltages) to achieve maximum sensitivity. Mass accuracy of recorded ions (vs. calculated) was ±10 millimass units (mmu, without internal calibration).

Analyses were run using full MS (50-1000 *m/z* range), MS^2 and MS^3 acquisition in the positive ion mode, with a resolution of 30000 (500 *m/*z FWHM) in FTMS mode. The ions submitted to MS^n acquisition were chosen on the basis of full MS spectra abundance, without using automatic dependendent scan. Collision energy was set to 30 (arbitrary units) for all of the MS^n acquisition methods. The MS^n acquisition range was between the values of ion trap cut-off and the *m/z* of the fragmented ion. Xcalibur (Thermo Scientific, Milan, Italy) software was used for both acquisition and elaboration.

Ion chromatography

A Dionex instrument was employed, with eluent conductivity suppression and conductometric detection. Ammonium ions were determined with a CS12A column and 25 mM metansulfonic acid as eluent, at a flow rate of 1 mL/min. In such conditions the retention time of ammonium was 4.7 min. The anions were analyzed with an AS9HC anionic column and a mobile phase composed of $NaHCO_3$ 12 mM and K_2CO_3 5 mM, at a flow rate of 1 mL/min. In these conditions the retention times of nitrite and nitrate were 8.30 and 9.58 min, respectively.

Total organic carbon analysis

Total organic carbon (TOC) was measured on filtered suspensions using a Shimadzu TOC-5000 analyzer (catalytic oxidation on Pt at 680°C). The calibration was performed using standards of potassium hydrogen phthalate.

Toxicity Measurements

The toxicity of samples collected at different irradiation times was evaluated with a Microtox Model 500 Toxicity Analyzer (ECOTOX, Milan, Italy). Acute toxicity was determined with a bioluminescence inhibition assay using the marine bacterium *Vibrio fischeri*, monitoring changes in the natural emission of the luminescent bacteria when challenged with toxic compounds. Freeze-dried bacteria, reconstitution solution, diluent (2% NaCl) and an adjustment solution (non-toxic 22% sodium chloride) were obtained from Azur (Milan, Italy). Samples were tested in five dilutions in a medium containing 2% sodium chloride, and luminescence was recorded after 5, 15 and 30 min of incubation at 15^{o} C. Since no substantial differences were found between the three contact times, hereafter the results related to 5 minutes of contact are reported. Inhibition of luminescence, compared to a toxic-free control to give the percentage inhibition, was calculated following the established protocol using the Microtox calculation program.

Photochemical modeling

The assessment of the phototransformation kinetics of EMIM in sunlit natural waters was carried out with the APEX software (Aqueous Photochemistry of Environmentally-occurring Xenobiotics).[24] It predicts photochemical half-life times as a function of water chemistry and depth, for compounds with known direct photolysis quantum yields and second-order reaction rate constants with transient species.[26] APEX is based on a photochemical model, validated by comparison with field data of phototransformation kinetics in surface freshwaters.[27,28,29]

APEX results apply to well-mixed water bodies, including the epilimnion of stratified lakes. The absorption of radiation by photosensitisers (chromophoric dissolved organic matter, nitrate and nitrite) and xenobiotics is computed by taking into account competition for sunlight irradiance in a Lambert-Beer approach. Data obtained with APEX are averages over the water column of given depth, and they include the contributions of the well-illuminated surface layer and of darker water at

the bottom. Therefore, results as a function of depth are not depth profiles, but rather the comparison between different water bodies.

Sunlight irradiance is not constant in the natural environment, because of meteorological issues (not included in APEX) and of diurnal and seasonal cycles. To allow easier comparison between model results and environmental conditions, APEX uses as time unit a summer sunny day (SSD), equivalent to fair-weather 15 July at 45° N latitude. Another issue is that sunlight is not vertically incident over the water surface, but refraction at the interface deviates the light path in water towards the vertical. The light path length l depends on the depth d: on 15 July at 45°N it is $l = 1.05\ d$ at noon and $l = 1.17\ d$ at ±3 h from noon, which is a reasonable daily average.[24]

Results and Discussion

Ionic liquids disappearance, acute toxicity and mineralization

The addition of TiO_2 enhanced the photodegradation of both HMIM and EMIM, allowing their complete disappearance to be achieved within 2 hours of irradiation (Figure 1). The disappearance kinetics of the two compounds was very similar. Considering that EMIM at pH 7 would occur as the protonated (cationic) form, while HMIM would be a mixture of the protonated and the neutral one, the photocatalytic reactivity is probably similar for the two forms. While the imidazole could be easier to oxidize, the degradation of the imidazolium might be enhanced by the electrostatic interaction with TiO_2 (negatively charged at pH 7).[25]

Figure 1 also reports the TOC time trend. After complete disappearance of EMIM and HMIM only 50% of the TOC was removed, which suggested the occurrence of organic TPs. For both compounds, almost complete mineralization was achieved after 4 hours of irradiation.

Organic nitrogen was mainly transformed into ammonium (about 90%) and only for a small part into nitrate (10%), in agreement with literature data concerning the fate of organic nitrogen in photocatalysis.[30] It is known that for heterocyclic compounds containing a -N=C- portion, the main degradation product originated by nitrogen is NH_4^+, while NO_3^- is formed to a lesser extent.

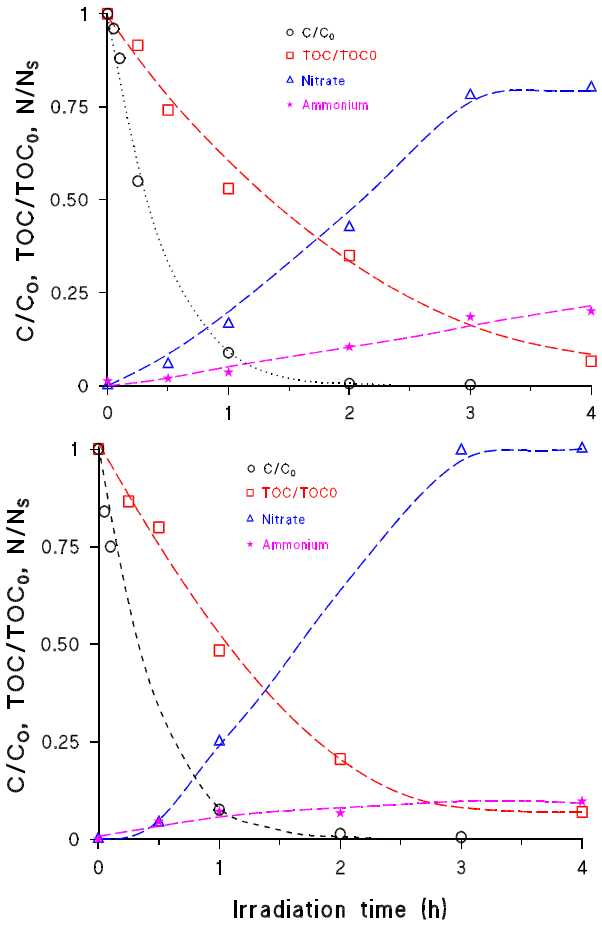

Figure 1. ILs disappearance, TOC profile and evolution of inorganic ions as a function of irradiation time, in the presence of TiO_2-P25. Top: HMIM; bottom: EMIM.

Acute toxicity was evaluated with *Vibrio fischeri* bacteria and it is expressed as the percentage of inhibition of the bacteria luminescence. Results obtained on samples subjected to heterogeneous photocatalysis are plotted in Figure 2. The two ILs were tested at a concentration of 10 mg/L, well below their EC50 dose (8.13×10^{-4} M for HMIM and 2.14×10^{-2} M for EMIM [23,31]), yielding very low initial toxicity. However, their transformation proceeded through the production of harmful compounds and the inhibition of luminescence increased from 30 min onwards, reaching up to 70%. This issue suggests the formation of TPs with higher toxicity than the parent molecules. Interestingly, for both compounds under irradiation, the toxicity reached a maximum after two hours and then decreased, with almost no residual toxicity after 4 hours. This is in tune with the almost complete mineralization at the same time scale.

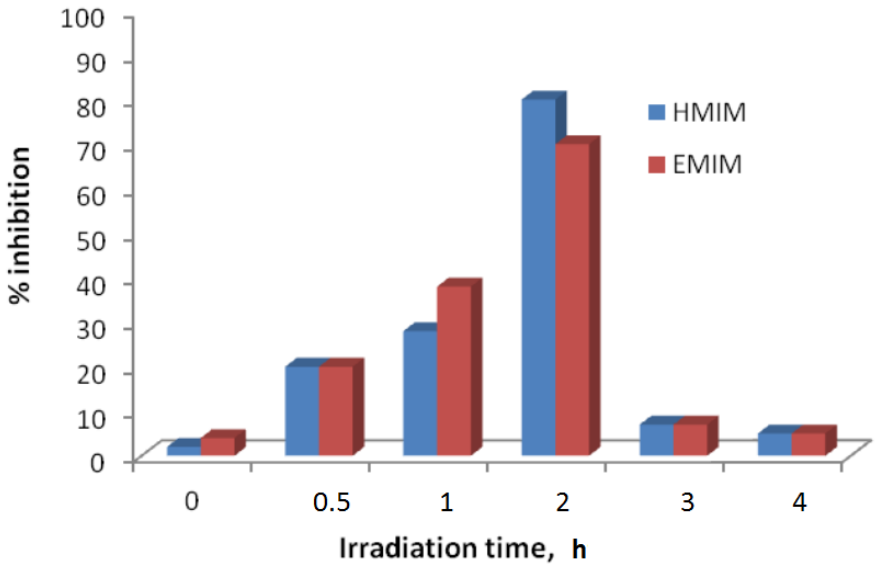

Figure 2. Acute toxicity of HMIM and EMIM as a function of the irradiation time, in the presence of TiO_2-P25.

TPs formation

The search for TPs formed from HMIM and EMIM was performed through HPLC-HRMS. HMIM has 83.0603 *m/z*, while EMIM has 111.0947 *m/z*. The ESI+ mass spectra of the TPs were useful means for the determination of their molecular mass, and the high resolving power was essential to attribute empirical formulae within the Orbitrap working range (≥ 50 *m/z*). Spectra involving ions with *m/z* < 50 were acquired with the linear ion trap only, at low resolution. Accurate HRMS *m/z* values of the parent ions are reported with errors below 1 mmu, which guarantees the correct assignment of molecular formulae in all cases. The MS^2 spectra showed several structural-diagnostic ions that allowed the characterization of the different TPs and the distinction between isobaric species. In order to maximize the signals, the samples for LC-HRMS runs were prepared using a 20-times higher concentration of ILs compared to the HPLC-UV experiments.

TPs of HMIM

Five transformation products (TPs) were formed upon HMIM disappearance. Accurate *m/z* ratios, retention times and MS^2 product ions are listed in Table S1 in the Supporting Information (hereafter SI), while their profiles of formation and disappearance are shown in Fig. S1(SI). All TPs followed a similar evolution profile with simultaneous formation, and many of them reached concentration maxima after 2 h irradiation.

Two species with 117.0670 *m/z* and empirical formula $C_4H_9O_2N_2$ were detected, which were likely formed through hydroxylation and addition of a molecule of water. Both species share the same MS^2 product ions, although with different relative abundances. The MS^2 spectrum of **117-B** shows three product ions (see Fig. S2(SI)): 99.0585 *m/z* as base peak, involving the loss of a water molecule, the peak 72.0464 *m/z*, resulting from the loss of CH_3ON, as well as the very diagnostic ion at 58.0303 *m/z*, resulting from the loss of C_2H_5ON. The formation of the latter two ions would be well-matched with the detachment of the aminomethylen moiety plus an oxygen and, therefore, with an hydroxylation of the methyl group. Furthermore, the loss of a C_2H_5ON molecule could take place only if the addition of the second OH group occurred on the N3 (**117-A**) or C4 (**117-B**) atom.

The formation of the other three TPs probably involved the imidazole ring opening. The species with 72.0460 *m/z* and empirical formula C_3H_6ON should be N-ethylenformamide. The MS^2 spectrum showed the formation of a product ion at 44 *m/z*, due to the possible loss of a molecule of carbon monoxide (see Scheme 1). The formation of this compound was confirmed by the injection of a commercially available standard. Reasonably, N-ethylenformamide underwent hydroxylation producing the TP at 88.0415 *m/z*, with molecular formula $C_3H_6NO_2$. Unfortunately no product ions were detected in the MS^2 study, which prevented the confirmation of the structure of the latter TP.

The species with 60.0457 *m/z* and empirical formula C_2H_6ON is the main TP by peak area, and it was tentatively attributed to ethylene hydroxylamine. The MS^2 analysis showed the loss of a water and an ethylene molecule, which is well matched with the proposed structure.

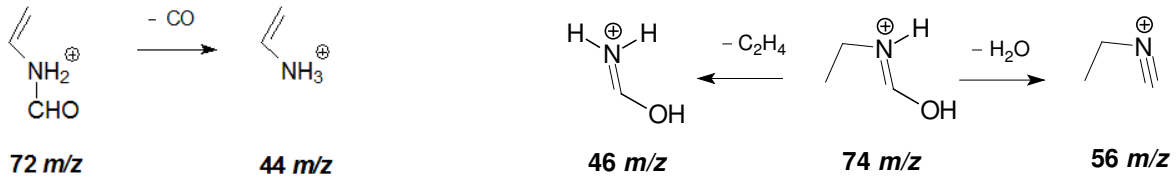

Scheme 1. *Left*: Proposed fragmentation pathways followed by TP **72** (HMIM). *Right*: Proposed fragmentation pathways followed by TP **74** (EMIM).

TPs of EMIM

The MS^2 spectrum of EMIM highlighted the formation of a main product ion at 83.0603 *m/z*, resulting from the loss of ethylene, as shown in Fig. S3(SI). Nine TPs were detected; their relevant data are listed in Table S2(SI), while the time evolution profiles are plotted in Fig. S4(SI). Again,

all TPs followed a similar evolution with simultaneous formation and final disappearance.

Two species with 145.1026 *m/z* and empirical formula $C_6H_{13}O_2N_2$ were detected and attributed to hydroxylation/water addition processes. In close analogy with HMIM, also in this case one can assume hydroxylation of the ethyl chain, while the addition of water would involve the imidazole double bonds. The MS^2 spectra of **145-A** and **145-B** show the formation of the same three major product ions: 72.0449 *m/z*, originated from the loss of C_3H_9NO, 86.0605 *m/z*, originated from the loss of C_2H_7NO, and 127.0871 *m/z* due to loss of a water molecule (see Fig. S5(SI)). The formation of these ions allowed to tentatively place one of the two hydroxyl groups on the ethyl chain and the other one on the imidazole ring. The two isomers differ for the location of the latter hydroxylation, which in one case would be on the C4 atom and in the other on N3.

A TP with 127.0797 *m/z* and empirical formula $C_6H_{11}ON_2$ was also detected. Its MS^2 spectrum highlights two main fragmentation pathways, due to two different cleavages of the imidazole ring. The product ion at 72.0449 *m/z* was formed through the loss of methylethylamine (C_3H_5N), while the ion at 86.0605 *m/z* is due to the loss of a molecule of ethylamine (C_2H_5N). These typical losses exclude an hydroxylation of the alkyl chains, supporting the hypothesis that the hydroxyl group would be located on the imidazole ring (see Fig. S6(SI)). The species at 125.0750 *m/z*, with empirical formula $C_6H_9ON_2$, is well matched with a hydroxylated/oxidized derivative. The formation of the product ion at 97.0765 m/z in the MS^2 spectrum, through the loss of CO, allows the assessment of the oxidation of the methyl group (see Fig. S7(SI)).

Five TPs were formed through the imidazole ring opening. Three of them were already recognized during HMIM degradation, namely 88.0415, 72.0460 and 60.0457 *m/z*. In addition, a TP with 102.1287 *m/z* and empirical formula $C_4H_8O_2N$ was formed through ring cleavage. The MS^2 spectrum presents the product ion 84.0449 *m/z*, due to the loss of a water molecule, and the ion 74.0605 *m/z*, formed by CO loss. The structure shown in Scheme 2 can thus be proposed:

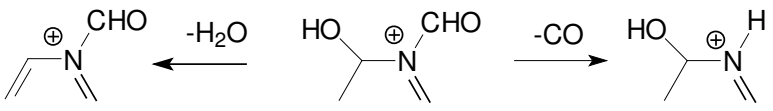

Scheme 2. Proposed fragmentation pathways followed by the TP at 102.1287 *m/z*.

The species 74.0968 *m/z*, with empirical formula C_3H_8ON, shows in its MS^2 spectrum the formation of the product ion 56.0500 *m/z*. This ion results from the loss of a water molecule while the ion with

46 *m/z*, probably due to the loss of ethylene, is well matched with the structure shown in Scheme 1.

Transformation pathways for HMIM and EMIM

Based on the identified TPs and given their profiles of formation/disappearance, a possible mechanism of transformation for the two ionic liquids is tentatively proposed in Scheme 3.

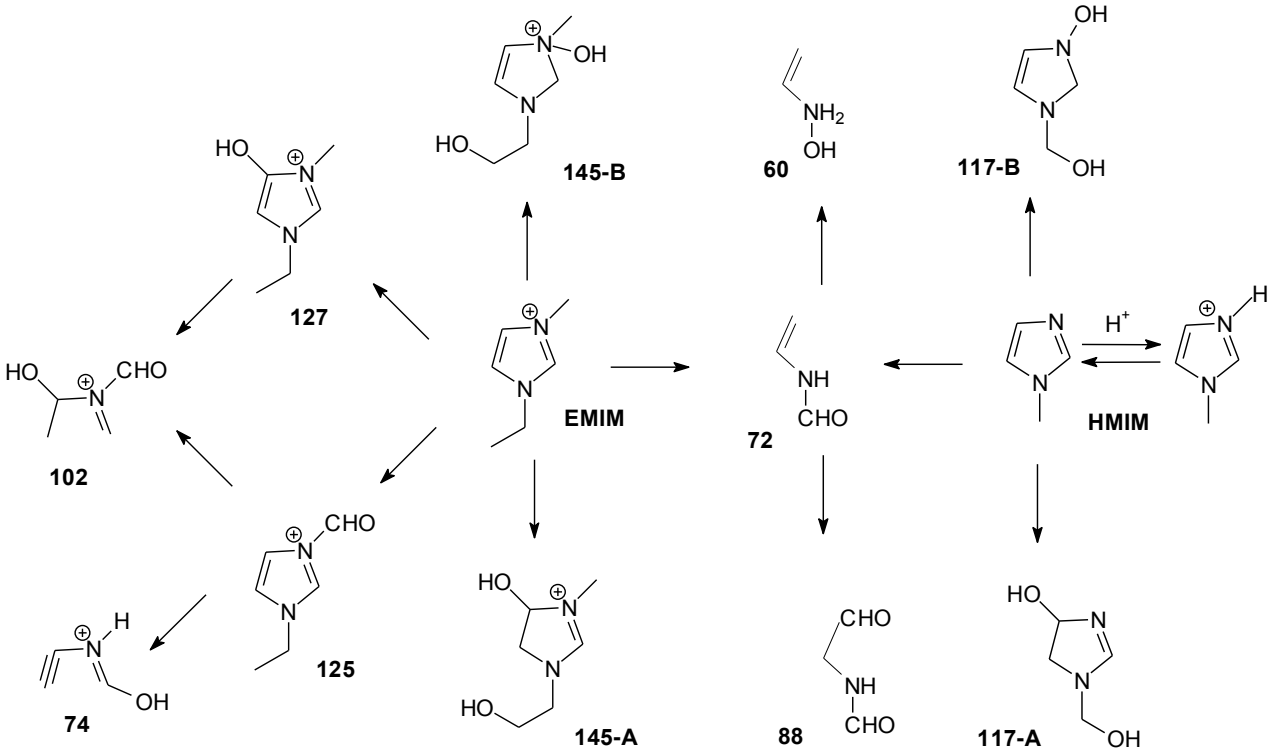

Scheme 3. Main transformation pathways proposed for HMIM and EMIM.

In the case of HMIM, three simultaneous processes would occur: two of them would involve dihydroxylation (yielding **117-A**, **117-B**) and another one the imidazole ring cleavage, presumably producing N-hydroxyvinylamine (**60**), ethylenformamide (**72**) and hydroxyethylenformamide (**88**). In the case of EMIM, dihydroxylation would yield **145-A** and **145-B** while single hydroxylation would produce **125** and **127**. Additional pathways presumably involved the cleavage of the imidazole ring to give **74** (presumably from **125**) and **102** (from **127**), as well as direct ring breaking from EMIM to give **60**, **72** and **88**, which EMIM shares with HMIM as TPs.

Interestingly, the formation of several N-formyl compounds[32] might potentially account for the increase of toxicity that was observed under photocatalytic conditions, before complete mineralization.

Modeling of EMIM phototransformation in surface waters

Photochemical reactivity data were obtained for EMIM under neutral pH conditions, following an established experimental protocol.[26,27,28] The experimental procedures used for the measurement of the photoreactivity parameters are reported in the SI (see Figures S8-S13 and related text). It was obtained a direct photolysis quantum yield Φ_{EMIM} = 0.117±0.010, as well as the second-order reaction rate constants with $^{\bullet}OH$, $^{1}O_2$ and ^{3}AQ2S* (the latter taken as ^{3}CDOM* proxy), respectively $k_{EMIM,\bullet OH}$ = (2.1 ± 0.3)·10^{10} M^{-1} s^{-1}, $k_{EMIM,1O2}$ = (8.5±3.0)·10^{5} M^{-1} s^{-1}, and $k_{EMIM,3AQ2S*}$ = (2.7±0.2)·10^{8} M^{-1} s^{-1}. Additionally note that reaction between EMIM and $CO_3^{-\bullet}$ would be negligible in surface waters (see SI). From these data one gets that the reactivity with $^{\bullet}OH$ is near the diffusion limit, while that with $^{1}O_2$ is quite low. The fact that $k_{EMIM,3AQ2S*} \ll k_{EMIM,\bullet OH}$ is offset by the fact that [^{3}CDOM*] » [$^{\bullet}OH$] in surface water, the extent of which will be assessed by modeling. A similar issue holds for the (relatively high) value of Φ_{EMIM}.

The APEX-modeled half-life time of EMIM (units of SSD = summer sunny days equivalent to 15 July at 45°N latitude), as a function of water depth and of the dissolved organic carbon (DOC) content, is reported in Figure S14(SI). The results suggest that EMIM would be quite photolabile in surface waters during summertime: its half-life time would vary from less than one day under the conditions most favorable to photodegradation (low DOC and/or low depth) to less than a couple of weeks at 15 mg C L^{-1} DOC and 10 m depth.

Figure 3 reports, as a function of DOC and for a fixed 5 m water depth, the modeled percentage of EMIM phototransformation accounted for by the main photoprocesses. It is shown that the direct photolysis would be the prevailing pathway, accounting for 60-90% of photodegradation, followed by reactions with $^{\bullet}OH$ (up to ~40%) and with ^{3}CDOM* (up to 2.5%). Note that $^{1}O_2$ and $CO_3^{-\bullet}$ would play a negligible role in EMIM phototransformation. Because direct photolysis would be the prevailing photoprocess for EMIM, the most important water parameters that control its transformation would be water depth and DOC. Other parameters (nitrate, nitrite, carbonate, bicarbonate) would be less important.

To further demonstrate the importance of direct photolysis in EMIM phototransformation, irradiation experiments were carried out with 20 µM EMIM spiked to ultra-pure water and to lake water (see Figure S15 in SI). Surface water was sampled from the epilimnion of two lakes located in the Torino province (NW Italy), namely lakes Avigliana and Candia.[33] If direct photolysis were the main transformation process, photodegradation would be about as fast in ultra-pure water as in

lake water (or even faster, because the photoactive components of lake water compete with the substrate for lamp irradiance). This assumption was confirmed, consistently with the expected importance of EMIM direct photolysis. Note, however, that the results of laboratory experiments alone may not be sufficient or adequate to prove the importance of direct *vs.* indirect photochemistry in the natural environment.[34] In this work, laboratory results are in agreement with modeling data, which adds to the significance of both.

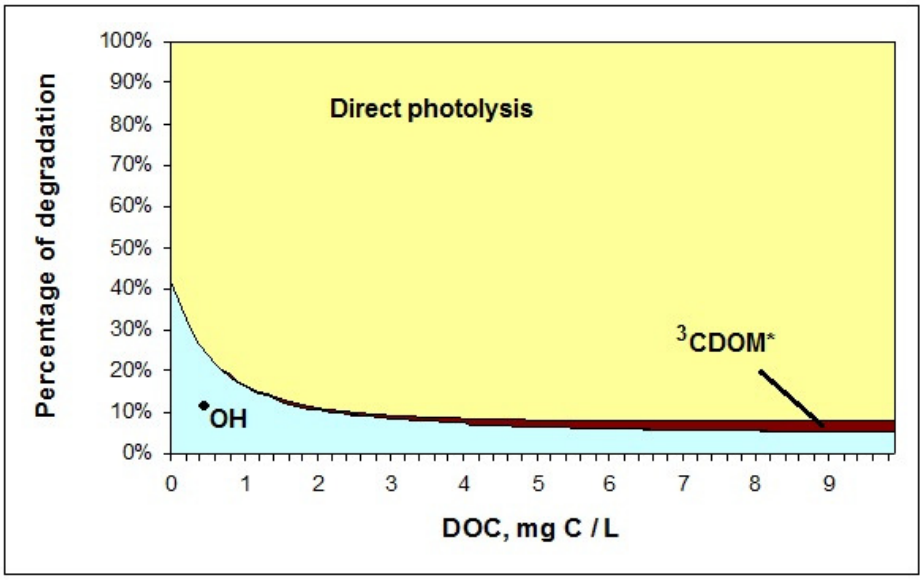

Figure 3. Modeled percentage of EMIM phototransformation accounted for by direct photolysis and reactions with •OH and ^{3}CDOM*, under summertime irradiation conditions, as a function of the DOC. Other water conditions: 5 m depth, 0.1 mM nitrate, 1 µM nitrite, 1 mM bicarbonate, 10 µM carbonate.

As shown in Figure 3, the process involving ^{3}CDOM* shows an increasing relative importance with increasing DOC, because high-DOC waters contain elevated CDOM that is the direct source of ^{3}CDOM*. In contrast, the •OH process is inhibited with increasing DOC because DOM is an important •OH scavenger.[35,36,37,38]

The results reported so far have been obtained by assuming summertime irradiation conditions. To assess the phototransformation of EMIM in different periods of the year, it was used the *Apex_season* function of the APEX software that, in combination with the *APEX_errors* function,[24] yielded the results reported in Figure 4. Under the assumed conditions (5 m depth and DOC = 5 mg

C L^{-1}), the half-life time would vary from a few days in summer to around one month in winter. Still, even under wintertime irradiation, EMIM could not be considered as a persistent pollutant in surface waters.

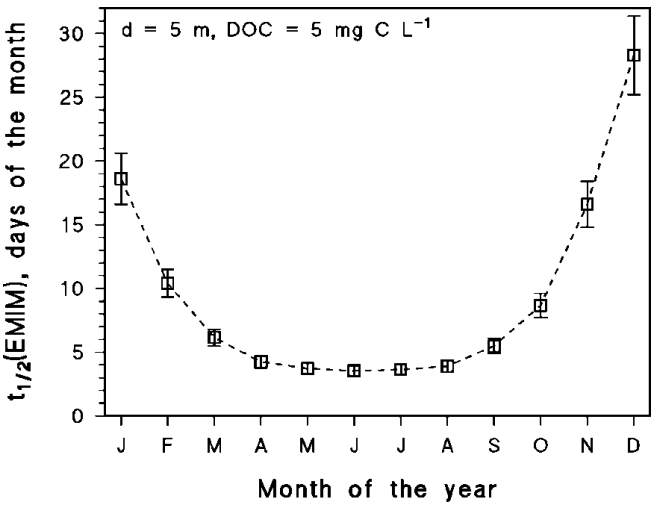

Figure 4. Half-life time of EMIM in different months of the year (the time unit is days of the relevant month). Water conditions: 5 m depth, 5 mg C L^{-1} DOC, 0.1 mM nitrate, 1 μM nitrite, 1 mM bicarbonate, 10 μM carbonate. The error bounds to the data represent ±σ.

Technological and Environmental Implications

Heterogeneous photocatalysis is a potentially effective technique for the degradation of HMIM and EMIM. Under the studied conditions, complete disappearance of the two compounds was obtained in two hours irradiation, but several potentially toxic TPs would still occur. The detected TPs would likely be produced through hydroxylation, oxidation and ring-opening. However, a further two hours irradiation (more, in case of higher substrate concentration) were sufficient to achieve complete mineralization, thereby allowing complete decontamination. Further work will need to take into account the effects of natural water and wastewater components on the photocatalytic degradation kinetics.

If released into surface water bodies because of insufficient treatment, EMIM would be poorly persistent from a photochemical point of view. Its environmental photodegradation would be mostly accounted for by direct photolysis and, to a lesser extent, by reaction with $^{\bullet}$OH. Processes induced

by ^{3}CDOM* would play a minor role, while reactions with $^{1}O_2$ and $CO_3^{-\bullet}$ would be negligible. In temperate regions under fair-weather conditions, the half-life time of EMIM would range from a few days in summertime to about one month in winter. Despite the elevated potential for the photochemical attenuation of EMIM in surface-water environments, the possible formation of toxic intermediates is an issue that needs consideration. Indeed, the degradation of pollutants by means of TiO_2-based photocatalysis has been shown to be a good predictor for the formation of TPs *via* photochemical processes in the natural environment.[39,40,41]

Acknowledgments

C.M. acknowledges financial support by the NANOMED project (PRIN 2010-2011, 2010FPTBSH_003) from the Italian Ministero dell'Istruzione, dell'Università e della Ricerca (MIUR). D.V. acknowledges support by Università di Torino / Compagnia di San Paolo - EU Accelerating Grants, project TO_Call2_2012_0047 (DOMNAMICS). P.C., D.F. and D.V. acknowledge support by MIUR, in the frame of the collaborative international consortium WATERJPI2013-MOTREM of the "Water Challenges for a Changing World" Joint Programming Initiative (WaterJPI) Pilot Call.

References

(1) Richardson, S. D.; Ternes, T. A. Water analysis: emerging contaminants and current issues. *Anal. Chem.* **2011**, *83*, 4614-4648.

(2) Earle, M. J.; Seddon, K. R. Ionic liquids. Green solvents for the future. *Pure Appl. Chem.* **2000**, *72*, 1391-1398.

(3) Kalcikova, G.; Zagore-Koncan, J.; Znidarsic-Plazi, P.; Gotvajn, A. Z. Assessment of environmental impact of pyridinium-based ionic liquid. *Fresenius Environ. Bull.* **2012**, *21*, 2320-2325.

(4) Jastorff, B.; Stormann, R.; Ranke, J.; Molter, K.; Stock, F. F.; Oberheitmann, B.; Hoffmann, W.; Nuchter, M.; Ondruschka, B.; Filser, J. J. How hazardous are ionic liquids? Structure-activity relationships and biological testing as important elements for sustainability evaluation. *Green Chem.* **2003**, *5*, 136-142.

(5) Matzke, M.; Stolte, S.; Thiele, K.; Juffernholz, T.; Arning, J.; Ranke, J.; Welz-Biermann, U.; Jastorff, B. The influence of anion species on the toxicity of 1-alkyl-3-methylimidazolium ionic liquids observed in an (eco)toxicological test battery. *Green Chem.* **2007**, *9*, 1198-1207.

(6) Ranke, J.; Stolte, S.; Störmann, R.; Arning, J.; Jastorff, B. Design of sustainable chemical products – the example of ionic liquids. *Chem. Rev.* **2007**, *107*, 2183-2206.

(7) Stolte, S.; Matzke, M.; Arning, J.; Böschen, A.; Pitner, W. R.; Welz-Biermann, U.; Jastorff, B.; Ranke, J. Effects of different head groups and functionalised side chains on the aquatic toxicity of ionic liquids. *Green Chem.* **2007**, *9*, 1170-1179.

(8) Pretti, C.; Chiappe, C.; Pieraccini, D.; Gregori, M.; Abramo, F.; Monni, G.; Intorre, L. Acute toxicity of ionic liquids to the zebrafish (*Danio rerio*). *Green Chem.* **2006**, *8*, 238-240.

(9) Pretti, C.; Chiappe, C.; Baldetti, I.; Brunini, S.; Monni G. Acute toxicity of ionic liquids for three freshwater organisms: *Pseudokirchneriella subcapitata*, *Daphnia magna* and *Danio rerio*. *Ecotoxicol. Environ. Safety* **2009**, *72*, 1170-1176.

(10) Matzke, M.; Stolte, S.; Arning, J.; Uebers, U.; Filser J. Imidazolium based ionic liquids in soils: effects of the side chain length on wheat (*Triticum aestivum*) and cress (*Lepidium sativum*) as affected by different clays and organic matter. *Green Chem.* **2008**, *10*, 584–591.

(11) Larson, J. H.; Frost, P. C.; Lamberti, G. A. Variable toxicity of ionic liquid forming chemicals to *Lemnia minor* and the influence of dissolved organic matter. *Environ. Toxicol. Chem.* **2008**, *27*, 676-681.

(12) Luo, Y. R.; Wang, S. H.; Yun, M. X.; Li, X. Y.; Wange, J. J.; Sun, Z. J. The toxic effects of ionic liquids on the activities of acetylcholinesterase and cellulase in earthworms. *Chemosphere* **2009**, *77* 313-318.

(13) Swatloski, R. P.; Holbrey, J. D.; Memon, S. B.; Caldwell, G. A.; Caldwell, K. A.; Rogers, R.D. Using *Caenorhabditis elegans* to probe toxicity of 1-alkyl-3-methylimidazolium chloride based ionic liquids. *Chem. Commun.* **2004**, 668-669.

(14) Li, X. Y.; Zhou, J.; Yu, M.; Wang, J. J.; Pei, Y. C. Toxic effects of 1-methyl-3-octylimidazolium bromide on the early embryonic development of the frog *Rana nigromaculata*. *Ecotox. Environ. Safety* **2009**, *72*, 552-556.

(15) Yu, M.; Li, S.; Li, X.; Zhang, B.; Wang, J. Acute effects of 1-octyl-3-methylimidazolium bromide ionic liquid on the antioxidant enzyme system of mouse liver. *Ecotoxicol. Environ. Safety* **2008**, *71*, 903– 908

(16) Costello, D. M.; Brown, L. M.; Lamberti, G. A. Acute toxic effects of ionic liquids on zebra mussel (*Dreissena polymorpha*) survival and feeding. *Green Chem.* **2009**, *11*, 548-553.

(17) Stepnowski, P.; Skladanowski, A. C.; Ludwiczak, A.; Laczynska, E. Evaluating the cytotoxicity of ionic liquids using human cell line HeLa. *Hum. Exp. Toxicol.* **2004**, *23*, 513-517.

(18) Stock, F.; Hoffmann, J.; Ranke, J.; Störmann, R.; Ondruschka, B.; Jastorff B. Effects of ionic liquids on the acetylcholinesterase – a structure–activity relationship consideration. *Green Chem.* **2004**, *6*, 286-290.

(19) Składanowski, A. C.; Stepnowski, P.; Kleszczyński, K.; Dmochowska, B. AMP deaminase in vitro inhibition by xenobiotics: A potential molecular method for risk assessment of synthetic nitro- and polycyclic musks, imidazolium ionic liquids and N-glucopyranosyl ammonium salts. *Environ. Toxicol. Phar.* **2005**, *19*, 291-296.

(20) Yu, M.; Wang, S. H.; Luo, Y. R.; Han, Y. W.; Li, X. Y.; Zhang, B. J.; Wang, J. J. Effects of the 1-alkyl-3-methylimidazolium bromide ionic liquids on the antioxidant defense system of *Daphnia magna*. *Ecotoxicol. Environ. Safety* **2009**, *72*, 1798-1804.

(21) Bernot, R. J.; Brueseke, M. A.; Evans-White, M. A.; Lamberti, G. Acute and chronic toxicity of imidazolium-based ionic liquids towards *Daphnia magna*. *Environ. Toxicol. Chem.* **2005**, *24*, 87-92.

(22) Couling, D.; Bernot, R.; Docherty, K.; Dixon, J.; Maginn, E. Assessing the factors responsible for ionic liquid toxicity to aquatic organisms via quantitative structure–property relationship modeling. *Green Chem.* **2006**, *8*, 82-90.

(23) Wells, A. S.; Coombe, V. T. On the freshwater ecotoxicity and biodegradation properties of some common ionic liquids. *Org. Proc. Res.* **2006**, *10*, 794-798.

(24) Bodrato, M.; Vione, D. APEX (Aqueous Photochemistry of Environmentally occurring Xenobiotics): A free software tool to predict the kinetics of photochemical processes in surface waters. *Environ. Sci.: Processes Impacts* **2014**, *16*, 732-740.

(25) Nakata, K.; Fujishima, A. TiO_2 photocatalysis: Design and applications. *J. Photochem. Photobiol. C: Photochem. Rev.* **2012**, *13*, 169-189.

(26) De Laurentiis, E.; Chiron, S.; Kouras-Hadef, S.; Richard, C.; Minella, M.; Maurino, V.; Minero, C.; Vione, D. Photochemical fate of carbamazepine in surface freshwaters: Laboratory measures and modeling. *Environ. Sci. Technol.* **2012**, *46*, 8164-8173.

(27) Vione, D.; Maddigapu, P. R.; De Laurentiis, E.; Minella, M.; Pazzi, M.; Maurino, V.; Minero, C.; Kouras, S.; Richard, C. Modelling the photochemical fate of ibuprofen in surface waters. *Water Res.* **2011**, *45*, 6725-6736.

(28) Marchetti, G.; Minella, M.; Maurino, V.; Minero, C.; Vione, D. Photochemical transformation of atrazine and formation of photointermediates under conditions relevant to sunlit surface waters: Laboratory measures and modelling. *Water Res.* **2013**, *47*, 6211-6222.

(29) Fabbri, D.; Minella, M.; Maurino, V.; Minero, C.; Vione, D. Photochemical transformation of phenylurea herbicides in surface waters: A model assessment of persistence, and implications for the possible generation of hazardous intermediates. *Chemosphere* **2015**, *119*, 601-607.

(30) Calza, P.; Pelizzetti, E.; Minero, C. The fate of the organic nitrogen in photocatalysis. An overview. *J. Appl. Electrochem.* **2005**, *35*, 665-673

(31) Ranke, J.; Molter, K.; Stock, F.; Bottin-Weber, U.; Poczobutt, J.; Hoffmann, J.; Ondruschka, B.; Filser, J.; Jastorff, B. Biological effects of imidazolium ionic liquids with varying chain lengths in acute *Vibrio fischeri* and WST-1 cell viability assays. *Ecotoxicol. Environ. Safety* **2004**, *58*, 396–404.

(32) Galichet, F.; Mailhot, G.; Bonnemoy, F.; Bohatier, J.; Bolte, M. Iron(III) photo-induced degradation of isoproturon: correlation between degradation and toxicity. *Pest. Manag. Sci.* **2002**, *58*, 707-712.

(33) Minella, M.; De Laurentiis, E.; Maurino, V.; Minero, C.; Vione, D. Dark production of hydroxyl radicals by aeration of anoxic lake water. *Sci. Total Environ.* **2015**, *527-528*, 322-327.

(34) Bianco, A.; Fabbri, D.; Minella, M.; Brigante, M.; Mailhot, G.; Maurino, V.; Minero, C.; Vione, D. New insights into the environmental photochemistry of 5-chloro-2-(2,4-dichlorophenoxy)phenol

(triclosan): Reconsidering the importance of indirect photoreactions. *Water Res.* **2015**, *72*, 271-280.
(35) Canonica, S.; Hellrung, B.; Müller, P.; Wirz, J. Aqueous oxidation of phenylurea herbicides by triplet aromatic ketones. *Environ. Sci. Technol.* **2006**, *40*, 6636-6641.
(36) McKay, G.; Dong, M. M.; Kleinman, J. L.; Mezyk, S. P.; Rosario-Ortiz, F. L. Temperature dependence of the reaction between the hydroxyl radical and organic matter. *Environ. Sci. Technol.* **2011**, *45*, 6932-6937.
(37) Keen, O. S.; McKay, G.; Mezyk, S. P.; Linden, K. G.; Rosario-Ortiz, F. L. Identifying the factors that influence the reactivity of effluent organic matter with hydroxyl radicals. *Water Res.* **2014**, *50*, 408-419.
(38) Vione, D.; Minella, M.; Maurino, V.; Minero, C. Indirect photochemistry in sunlit surface waters: Photoinduced production of reactive transient species. *Chemistry Eur. J.* **2014**, *20*, 10590-10606.
(39) Calza, P.; Marchisio, S.; Medana, C.; Baiocchi, C. Fate of the antibacterial spiramycin in river waters. *Anal. Bioanal. Chem.* **2010**, *396*, 1539-1550.
(40) Medana, C.; Calza, P.; Dal Bello, F.; Raso, E.; Minero, C.; Baiocchi, C. Multiple unknown degradants generated from the insect repellent DEET by photoinduced processes on TiO_2. *J. Mass Spectrom.* **2011,** *46*, 24-40.
(41) Calza, P., Medana, C., Padovano, E., Giancotti, V., Minero, C. Fate of selected pharmaceuticals in river waters. *Environ. Sci. Pollut. Res.* **2013**, *20*, 2262-2270.